Iron(0)-Catalyzed Hydrothermal Liquefaction of Switchgrass: the Effects of Co-Catalysts and Reductive Conditions

Fang Deng & Ananda S. Amarasekara

BioEnergy Research

ISSN 1939-1234

Bioenerg. Res.
DOI 10.1007/s12155-020-10140-9

Springer

BioEnergy Research
https://doi.org/10.1007/s12155-020-10140-9

Iron(0)-Catalyzed Hydrothermal Liquefaction of Switchgrass: the Effects of Co-Catalysts and Reductive Conditions

Fang Deng[1] · **Ananda S. Amarasekara**[1]

Abstract

The effects of a series of co-catalysts: iron(III)chloride, zinc chloride, sodium borate, acetic acid, oxalic acid, 10% Pd-C, sodium carbonate, and Raney-Ni as well as H_2 at 200 psi reductive conditions were studied on the iron(0)-catalyzed hydrothermal liquefaction of switchgrass at 210 °C. The addition 10% (w/w) iron(III)chloride as a co-catalyst in 60% aq. ethanol, without a hydrogen atmosphere enhanced the liquefaction yield from 55.7 ± 1.5 to 67.6 ± 2.5%. The use of Pd/C (5% w/w) and Raney-Ni (5% w/w) as co-catalysts could also enhance the liquefaction yields to 67.0 ± 3.0 and 72.3 ± 1.8% respectively, in reactions carried out under hydrogen atmosphere at 200 psi, in H_2O, 210 °C, 24 h. GC-MS analysis of the liquefaction products revealed that C5-C10 range partially oxygenated products are formed and the composition of the liquefaction product depends on the co-catalyst used. The thermogravimetric and FT-IR analysis of liquefaction residues indicated that polysaccharide fraction is mainly liquefied in these iron(0)-catalyzed liquefactions of switchgrass at 210 °C.

Keywords Biomass · Catalyst · Hydrogen · Iron powder · Bio-oil

Introduction

The biomass liquefaction in a solvent at a high temperature is another approach among a handful of currently studied approaches for the conversion of renewable carbon to a liquid fuel compatible to fossil fuels [1–3]. In general early biomass liquefaction, attempts were modeled after well-known World War II era coal liquefaction technologies. These early coal liquefaction technologies can be broadly divided into two groups: direct liquefaction and indirect liquefaction [4, 5]. The direct process is based on approaches such as carbonization, pyrolysis, and hydrogenation [5]. The indirect method usually involves gasification of coal or biomass to a mixture of carbon monoxide and hydrogen called syngas and then using Fischer-Tropsch chemistry for the conversion to liquid hydrocarbons [6]. The direct liquefaction is more straight-forward and requires a hydrogen-donor solvent or more often hydrogen gas at a high pressure as well as the proper catalytic system [7]. In most direct coal liquefaction, plant's coal is mixed with a hydrocarbon solvent and subjected to the hydrogenation at 400–500 °C, at a hydrogen pressure of 20–70 MPa in the presence of a catalysts [7, 8].

The use of water as a direct liquefaction medium has not gained traction in coal liquefaction, and this may be most likely due to incompatible solubility properties. However, there is a handful of attempts to use water as a co-solvent in coal liquefaction [9, 10]. On the other hand, water can be a better solvent for biomass with polar molecules capable of hydrogen bonding with water [11]. The hydrothermal liquefaction of biomass is a widely studied technique and generally carried out around 280–370 °C, and at pressures in the range 10 to 25 MPa [12–14]. Besides the use of water, a number of research groups have studied the use of organic solvents like ethanol, 1-octanol [15], polyhydric alcohols, phenol [16, 17], ethylene carbonate [18], and solvent mixtures [19] as the liquefaction medium. In many instances, the addition of a metal salt, acid, or a base as catalyst is known to improve the liquefaction bio-oil yield and lower the liquefaction temperature [20, 21]. Some of the catalysts tested in recent studies are K_2CO_3 [22], zeolites [23], $CuSO_4$ [19], Na_2CO_3 + Fe [24], Ni-Co/Al-Mg [25], $In(OTf)_3$, $Yb(OTf)_3$, $InCl_3$ [26], H_3BO_3, Al_2O_3 [27], $TiCl_4$ + $MgCl_4$ [28], Ni/Si-Al, Ni_2P [29], KF/Al_2O_3 [23], Co-Zn/HZSM-5 [30], and Ni/HZSM-5 [31].

Electronic supplementary material The online version of this article (https://doi.org/10.1007/s12155-020-10140-9) contains supplementary material, which is available to authorized users.

✉ Ananda S. Amarasekara
asamarasekara@pvamu.edu

[1] Department of Chemistry, Prairie View A&M University, Prairie View, TX 77446, USA

The use of iron-based catalysts is gaining attention in recent years for liquefaction of biomass in water and in other organic solvents [32–37]; in particular, iron salts $FeSO_4$ and $FeCl_3$ have shown excellent catalytic activities [21, 32, 38]. The use of iron as the liquefaction catalyst is a very attractive proposition due to a number of reasons such as (a) iron is the second most abundant metallic element on earth's crust and is the most inexpensive metal in the pure form, (b) iron is known to react with hot compressed water or steam according to the Eq. 1

$$3\,Fe + 4\,H_2O \rightleftarrows Fe_3O_4 + 4\,H_2 \tag{1}$$

producing in situ hydrogen for the reduction of the intermediates when water is used as the solvent, (c) recycling of iron oxide to Fe(0) is also possible with carbon as the reducing agent at high temperatures, and (d) iron is relatively less toxic than many other transition metals used in catalysis processes.

In this study, the effects of a series of co-catalysts and reductive conditions on the iron powder catalyzed liquefaction of untreated switchgrass were studied in an effort to develop an inexpensive catalytic method for producing renewable fuels from lignocellulosic biomass. Switchgrass was selected in particularly because the earlier work by de Caprariis et al. [37] on oak wood with relatively high lignin content of ~ 25% [39] resulted only about 40% liquefaction from experiments conducted at 260–320 °C, for 15 min. On the other hand, switchgrass with a relatively low lignin and high polysaccharide contents [40] can be expected to liquefy under milder conditions, and as far as we are aware, there are no reports of studies on the effect of addition of Fe(0) on the hydrothermal liquefaction of switchgrass. In addition, the effects of addition of a series of co-catalysts and the reductive conditions of a pressurized hydrogen atmosphere were also studied as attempts to improve the Fe(0) catalysis on bio-oil yield.

Experimental

Materials and Instrumentation

Switchgrass sample was collected at USDA-Agricultural Research Station at Lincoln, NE. Switchgrass from matured plants; dry whole plant sample was finely milled and sieved through a mesh (Aldrich mini-sieve set, Z 675415, size 25, particle size 0.7 mm) to obtain a homogeneous powder. The switchgrass powder was then air dried in a 70 °C oven for 15 h to achieve a constant weight and then stored in sealed glass bottles. The composition of switchgrass: cellulose and hemicellulose 80.4%; lignin 15.4%; ash 4.4% (w/w). Iron(III)chloride, iron powder (> 99%, 60 micron), zinc chloride, sodium borate, acetic acid, oxalic acid, palladium (10% w/w) on activated carbon, sodium carbonate, and Raney nickel (W.R. Grace Co. 2800 slurry in water) were purchased from Aldrich Chemical Co. Biomass samples were sonicated for 20 min. before liquefactions using a Sonics Virbra-Cell VCX130 sonicator at 130 W power. The switchgrass biomass liquefactions without the hydrogen atmosphere were carried out in 25-mL stainless steel solvothermal reaction kettles with Teflon inner sleeves, from Lonsino Medical Products Co. Ltd., Jingsu, China. The reactions were carried out by placing the sealed reaction vessel in a temperature-controlled oven (Cole-Palmer WU-52402-91) with ± 1 °C accuracy. High pressure switchgrass biomass liquefaction under hydrogen was conducted in a Parr Instrument Co. reactor with a 50-mL stainless-steel pressure vessel (4720) and a 4838 reactor controller. The reactor was pressurized to 120 psi and flushed with hydrogen three times before heating to the reaction temperature. The complete process using iron(0)-catalyzed hydrothermal liquefaction of switchgrass, with/without co-catalysts, hydrogen atmosphere, and preparation of the liquefaction product for GC-MS analysis is shown in the flow diagram in Fig. 1. The thermogravimetric analysis was carried out using a PYRIS Diamond TG-DTA system from PerkinElmer Inc. Chemical compositions of switchgrass samples and solid residuals were analyzed by using curve fitting data processing on OriginLab 2018b Graphing & Analysis software from OriginLab Corporation, Northampton, MA, USA [41, 42]. FT-IR spectra were recorded using Smiths IdentifyIR. The products were analyzed using gas chromatography-mass spectrometry (GC-MS) instrument with a Varian Saturn 2100 T gas chromatograph coupled to Varian 3900 mass spectrometer. The capillary column VF-5 ms (30 m × 0.25 mm I.D. coated with 0.25-µm film, NP:CP8944 Varian) was used. The GC conditions were as follows: the column temperature was programmed from 100 to 150 °C with a gradient of 10 °C/min; the injection temperature was 275 °C; helium was used as the carrier gas at a flow rate of 1.5 mL/min; and split ratio was 100. The mass analyzer operated at an electron impact energy of 70 eV. Mass spectra were recorded by scanning in the range 40 to 600 m/z. The compounds were identified by referring to NIST 98 library built into Varian MS Workstation version 6.9.2. software.

Liquefaction of switchgrass with iron(0)catalyst

The dried switchgrass powder (1.0 g) and iron(0) powder (2–20% w/w) was mixed with 10 mL of deionized water in a stainless steel solvothermal reaction kettle with Teflon inner sleeve and sonicated for 20 min. The reaction kettle was firmly closed and heated in an oven maintained at 210 °C for 6–24 h. After the reaction period, kettle was removed from the oven and immediately cooled under running cold water to quench the reaction. The contents were transferred into a centrifuge tube and centrifuged at 1700*g* for 15 min to precipitate the solids. The liquid phase was then extracted with methylene

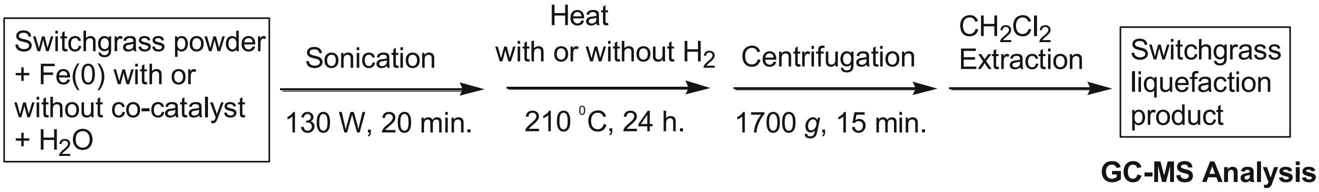

Fig. 1 Flow diagram for iron(0)-catalyzed hydrothermal liquefaction of switchgrass, with/without co-catalysts, hydrogen atmosphere, and preparation of the liquefaction product for GC-MS analysis

chloride (3 × 10mL), and the combined methylene chloride extract was used in the GC-MS analysis. The solid residue was dried in an oven at 95 °C for 24 h before weighing the dry biomass residue. This sample was used for thermogravimetric analysis (TGA) and IR analysis. The percent liquefaction was evaluated using the conversion ratio of switchgrass and calculated after a correction for the catalyst weight as follows:

$$\text{Percent liquefaction} = \frac{\text{Weight of dry switchgrass} - \text{Weight of dry biomass residue}}{\text{Weight of dry switchgrass}} \times 100\%$$

All experiments were carried out in duplicate. The percent liquefactions calculated were mainly applied for the comparisons of various catalysts as well as reaction conditions used in this work.

Liquefaction of Switchgrass with Iron(0) and a Co-Catalyst

The dried switchgrass powder (1.0 g), iron(0) powder (10% w/w), and co-catalyst (iron(III)chloride, zinc chloride, sodium borate, acetic acid, oxalic acid, 10% Pd-C, sodium carbonate or Raney-Ni; 10% w/w) was mixed with 10 mL of deionized water or 60% aqueous ethanol as the solvent in a stainless steel solvothermal reaction kettle with Teflon inner sleeves and sonicated for 20 min. The reaction kettle was firmly closed and heated in an oven maintained at 210 °C for 24 h. After the reaction period, the kettle was removed from the oven and processed as described in the previous procedure. The liquid phase was analyzed using GC-MS. The percent liquefaction was calculated using the equation in the previous procedure. All experiments were carried out in duplicates.

Liquefaction of Switchgrass with Iron(0) and a Co-Catalyst Under a Hydrogen Atmosphere

The dried switchgrass powder (1.0 g), iron(0) powder (10% w/w) and co-catalyst (10% Pd-C or Raney-Ni; 5% w/w) was mixed with 10 mL of deionized water in a Parr Instrument Co. reactor with a 50-mL stainless-steel pressure vessel (4720) and sonicated for 20 min. The stainless-steel vessel was flushed with hydrogen for three times and pressurized with hydrogen to 120 psi. The reactor temperature was gradually increased from room temperature to 210 °C in 30 min, held at 210 °C and at a pressure of 200 psi for 24 h. Then the reactor was cooled to room temperature and pressure released, and the content was processed as in the earlier procedure. The liquid phase was analyzed using GC-MS. The percent liquefaction was calculated as in earlier procedures; all experiments were carried out in duplicate.

Statistical Analysis

Statistical significance was detected by analysis of variance (ANOVA) and Tukey's honest significant difference (HSD) test at a 95% confidence level using SAS 9.4 software (SAS Institute Inc., Cary, NC, USA). For all variables with the same letter, the difference between the means is not statistically significant. If two variables have different letters, they are significantly different.

Results and Discussion

Switchgrass Liquefaction with Iron(0) as the Single Catalyst: the Effects of Catalyst Loading and Reaction Time

In the initial phase of experiments, iron powder was used as the single catalyst for hydrothermal liquefaction of switchgrass biomass; first, the effects of catalyst loading and the reaction time were studied. All liquefaction experiments were carried out at 210 °C, as literature examples have shown that similar hydrothermal liquefactions require temperatures above 200 °C to produce high liquefaction yields from lignocellulosic biomass forms [3]. The heat-up time of 7 min and cool down time of 3 min are negligibly small in comparison to total heating time of 24 h used in these experiments. The experiments with Fe(0) catalyst loadings at 2, 5, and 10% at 210 °C for 24 h resulted 47, 54, and 56% liquefactions. Further increase in catalyst loading to more than 10% failed to improve the liquefaction yield above 56%, and therefore all other experiments were carried out at 10% w/w Fe(0) catalyst loading. A baseline reference experiment without Fe(0) catalyst produced only less than 10% switchgrass liquefaction under similar conditions. The change in liquefaction yields with time was also studied using 10% w/w Fe(0) catalyst loading and at 210 °C. The result of this experiment is shown as Fig. 2, and a rapid increase in liquefaction is seen in the first 6 h, and no further improvements in liquefactions are seen after about 24 h; therefore, all liquefactions including co-catalyst addition experiments were also carried out for 24 h.

The Effects of Adding a Co-Catalyst in the Iron(0) Catalyzed Liquefaction of Switchgrass

In the second phase, effects of adding various co-catalysts to iron(0)-catalyzed liquefaction of switchgrass in water and in 60% aqueous ethanol, without a hydrogen atmosphere and at 210 °C, 24 h, were studied. The results of these experiments are shown in Table 1. The addition of a co-catalyst such as metal salt or an organic acid was reported to be helpful in other types of biomass conversion processes due to the lowering of the activation energy as well as changes in acidity in the catalyst system [43–45]. The first entry in this table is the iron(0)-catalyzed liquefaction of switchgrass without adding a co-catalyst. The majority of co-catalysts tested failed to improve the liquefaction yield and produced only retardation in liquefactions. However, the addition of 10% w/w iron(III)chloride in water produced a slight increase in the liquefaction yield from 55.7 ± 1.5 to 60.2 ± 2.1% as shown in entry 3. In an attempt to further enhance the liquefaction, 10% w/w iron(III)chloride co-catalyst was tested in 60 % aqueous ethanol, and this experiment produced the highest liquefaction yield of 67.6 ± 2.5% as shown in entry 4. This improvement in liquefaction may be due to the acidity provided by $FeCl_3$ in aqueous ethanol promoting the decomposition of amorphous hemicellulose as well as lignin due to chelation with Fe(III) ions. Meanwhile, disordered morphology such as disrupted ridged structure, loosen cracks, and pores, were also reported after iron(III)chloride with ethanol treatment other biomass forms, which are also beneficial for the liquefaction process [46].

Iron(0)-Catalyzed Liquefaction of Switchgrass Under a Hydrogen Atmosphere with and Without a Co-Catalyst

Next, the iron(0)-catalyzed liquefaction of switchgrass under a hydrogen atmosphere at 200 psi with and without a co-catalyst was studied using a Parr reactor. The results of these experiments are shown in Table 2. The reductive conditions under a hydrogen atmosphere significantly improved the liquefaction yield of switchgrass as shown in Table 2. In comparison, the experiment carried out without a hydrogen atmosphere, 10% w/w iron catalyst produced a 55.7 ± 1.5% liquefaction (entry 1,

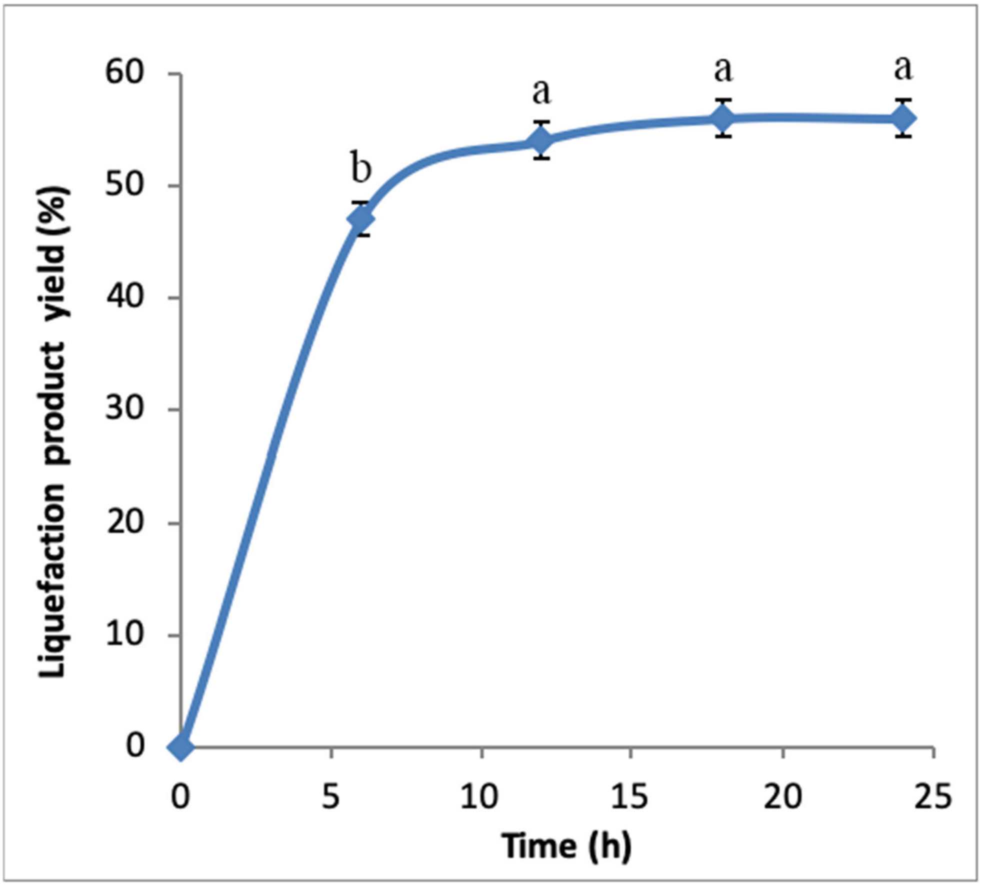

Fig. 2 The changes in switchgrass biomass liquefaction product percent yields with reaction time in the liquefaction time optimization experiment. Switchgrass (1.0 g) and Fe(0) (10% w/w) and 10 mL of water at 210 °C were used. Statistical significance is denoted by different letters a and b

Table 1 The effects of adding a co-catalyst in the iron(0)-catalyzed liquefaction of switchgrass. Switchgrass (1.0 g) and Fe(0) (10% w/w) and 10 mL of solvent at 210 °C, 24 h. Statistical significance is denoted by different letters a,b, and c

Entry	Co-catalyst and loading	Solvent	Percent liquefaction (% w/w)
1	-	H_2O	55.7 ± 1.5^{b}
2	Iron(III)chloride (2% w/w)	H_2O	51.8 ± 1.8^{bc}
3	Iron(III) chloride (10% w/w)	H_2O	60.2 ± 2.1^{ab}
4	Iron (III) chloride (10% w/w)	60% aq. EtOH	67.6 ± 2.5^{a}
5	Zinc chloride (2% w/w)	H_2O	47.8 ± 3.0^{c}
6	Sodium borate (2% w/w)	H_2O	47.4 ± 1.6^{c}
7	Acetic acid (2% w/w)	H_2O	50.8 ± 1.8^{bc}
8	Oxalic acid (2% w/w)	H_2O	46.2 ± 1.5^{c}
9	Pd/C (2% w/w)	H_2O	51.3 ± 1.6^{bc}
10	Sodium carbonate (2% w/w)	H_2O	49.7 ± 0.6^{bc}
11	Raney nickel (2% w/w)	H_2O	42.6 ± 1.8^{c}

Table 1); whereas the experiment under a hydrogen atmosphere with same catalyst loading and temperature produced a 69.2 ± 1.8% liquefaction (entry 1, Table 2). The addition of Pd/C or Raney-Ni as co-catalyst to liquefaction under a hydrogen atmosphere was also tested, and the results are shown as entries 2 and 3 in Table 2. The Pd/C (5% w/w) as co-catalyst had no significant effect on the liquefaction yield; whereas, the addition of Raney-Ni (5% w/w) as a co-catalyst under reductive conditions produced a statistically border line enhancement in liquefaction yield to reach 72.3 ± 1.8%, which is the highest yield of all experiments, as shown in entry 3 in Table 2.

GC-MS Analysis of Liquefaction Products from Iron(0)-Catalyzed Liquefaction of Switchgrass Under a Hydrogen Atmosphere with and Without a Co-Catalyst

The liquefaction products from iron(0) catalyzed liquefaction of switchgrass under a hydrogen atmosphere with and without a co-catalyst was analyzed using GC-MS in order to understand the composition of the oils formed. A comparison of GC-MS profiles of liquefaction products from iron(0)-catalyzed liquefaction of switchgrass under a hydrogen atmosphere with and without a co-catalyst is shown in Table 3. The GC-MS chromatograms are included in supplementary material of this article. Fourteen out of the 17 compounds founds were indentified in GC-MS analysis as shown in the fifth column in Table 3. The unidentified compounds eluting as peaks 4, 11, and 12 are labeled as unknowns. The peak number 5 eluting at 2.60 min in the chromatogram of liquefaction product produced using iron(0) catalysis without a co-catalyst showed the highest peak area percentage of 43.55%, and this compound with a formula $C_6H_6O_2$ was identified as 1-(2-furanyl) ethanone, commonly known as 2-acetyl furan. This peak was observed as peak with the highest peak area percentage (25.06%) in experiment with the addition of Pd/C (5% w/w) as a co-catalyst as well. However, the peak number 3 with retention time of 2.22 min is the compound with the highest peak area percentage (27.60%) in chromatogram of the liquefied product from experiment using Raney-Ni (5% w/w) as a co-catalyst. The proposed structure for this compound was eluting at 2.22 min with a formula $C_6H_{10}O$ is 2-methyl cyclopentanone. The majority of compounds in liquefied products and in particularly with six carbons and below are relatively smaller molecules generated from the degradation of cellulose and hemicellulose. Whereas peak numbers 13 to 17 are from phenolic compounds, most likely formed from the decomposition of lignin in switch grass. These aromatic and phenolic compounds together contribute to only about 20% of the total peak area in all three switchgrass liquefaction products under the mild conditions used in this work. In comparison, de Caprariis et al. [37] has recently reported the formation of a number of phenolic compounds from the lignin fraction and some carbonyl compounds from cellulose and hemicellulose during an iron catalyzed reductive hydrothermal liquefaction of oak wood biomass.

Table 2 Iron(0)-catalyzed liquefaction of switchgrass under a hydrogen atmosphere with and without a co-catalyst. Switchgrass (1.0 g) and 10 mL of water. The reactor temperature was increased from 23 to 210 °C in 30 min., held at 210 °C, pressure of 200 psi, H_2, 24 h., 210 °C. Statistical significance is denoted by letter a

Entry	Catalysts and loading	Percent liquefaction (% w/w)
1	Iron(0) (10% w/w)	69.2 ± 1.8^{a}
2	Iron(0) (10% w/w) + Pd/C (5% w/w)	67.0 ± 3.0^{a}
3	Iron(0) (10% w/w) + Raney Ni (5% w/w)	72.3 ± 1.8^{a}

Thermogravimetric Analysis of Switchgrass Biomass Residues After Iron(0)-Catalyzed Liquefactions

The effects of different iron(0)-catalyzed liquefactions on major components in switchgrass biomass, hemicellulose,

Table 3 A comparison of GC-MS profiles of liquefaction products from iron(0)-catalyzed liquefaction of switchgrass under a hydrogen atmosphere with and without a co-catalyst. Switchgrass (1.0 g) and 10 mL of water. The reactor temperature was increased from 23 to 210 °C in 30 min., held at 210 °C, pressure of 200 psi, H_2, 24 h

Peak	R_t (min)	m/z	Molecular formula	Possible compound	Catalyst		
					Iron(0) (10% w/w). Peak area (%)	Iron(0) (10% w/w) + Pd/C (5% w/w). Peak area (%)	Iron(0) (10% w/w) + Raney-Ni (5% w/w). Peak area (%)
1	2.00	84	C_5H_8O	Cyclopentanone	2.96	11.46	10.70
2	2.18	82	C_5H_6O	2-Cyclopenten-1-one	4.13	2.57	-
3	2.22	98	$C_6H_{10}O$	2-Methyl cyclopentanone	1.17	5.74	27.60
4	2.48	144	$C_8H_{16}O_2$	Unknown	-	7.72	4.73
5	2.60	110	$C_6H_6O_2$	1-(2- Furanyl) ethanone	43.55	25.06	4.27
6	2.63	112	$C_7H_{12}O$	2,5-Hexanedione	-	8.58	3.91
7	2.85	112	$C_7H_{12}O$	2-Propyl tetrahydrofuran	-	-	9.38
8	2.92	100	$C_5H_8O_2$	Dihydro-5-methyl 2(3H)-furanone	2.31	-	2.21
9	3.04	94	C_6H_6O	Phenol	5.00	4.13	4.27
10	3.29	110	$C_7H_{10}O$	2,3-Dimethyl 2-cyclopenten-1-one	9.94	6.17	-
11	3.55	112	$C_6H_8O_2$	Unknown	3.01	-	-
12	3.68	110	$C_7H_{10}O$	Unknown	3.14	2.67	2.75
13	4.19	124	$C_7H_8O_2$	2-Methoxy phenol	15.99	9.75	9.49
14	4.93	122	$C_8H_{10}O$	4-Ethyl phenol	1.42	7.78	8.24
15	6.12	152	$C_9H_{12}O_2$	4-Ethyl, 2-methoxy phenol	2.75	6.47	9.85
16	6.83	154	$C_8H_{10}O_3$	2,6-Dimethyoxy phenol	4.62	-	2.61
17	6.99	166	$C_{10}H_{14}O_2$	2-Methoxy, 4-propyl phenol	-	1.89	-

cellulose, and lignin were also studied. The residue left after liquefaction was separated and dried, and TGA was recorded as described in the experimental section. Then the derivative TGA curve data was analyzed by using OriginLab 2018b Graphing & Analysis software. The curve fitting software was used to determine the individual decomposition temperatures and the relative compositions of major components as described by others as well as in our previous work [41, 42, 47]. The TGA derivative curves as well as OriginLab 2018b curve fitting analysis for polysaccharides (hemicellulose and cellulose) and lignin components are included in the supplementary material of this article.

The effect of different iron(0)-catalyzed liquefactions on decomposition temperatures and compositions of major components in switchgrass biomass are shown in Table 4. In pure switchgrass, the decomposition temperatures of cellulose and hemicellulose are in the 297–322 °C range (entry 1). The polysaccharide (cellulose and hemicellulose) decomposition temperatures in all residues showed a shift towards lower temperatures as shown in Table 4 indicating the partial breakdown of polysaccharides due to iron(0)-catalyzed liquefactions. These shifts in polysaccharide decomposition temperatures from the average of hemicellulose and cellulose in pure switchgrass are shown in parenthesis in the third column of Table 4. The liquefactions 10% (w/w) Fe(0) + 5% Raney-Ni, H_2 at 200 psi, H_2O (entry 5), and 10% (w/w) Fe(0) + 10% (w/w) $FeCl_3$, H_2O (entry 6) produced the largest shifts in polysaccharide decomposition temperatures. The lignin decomposition temperatures and shifts from untreated switchgrass are shown in the fourth column. The liquefaction: 10% (w/w) Fe(0) + 5% Raney-Ni, H_2 at 200 psi, H_2O (entry 5) caused the highest shift in the lignin decomposition temperature, indicating the highest degradation in lignin structure during the liquefaction; interestingly, the highest liquefaction yield was also attained in this experiment. The percentage composition of polysaccharide and lignin in untreated switchgrass and liquefaction residues are shown in the last two columns of Table 4. The polysaccharide and lignin percentages of untreated switchgrass are 80.4 and 15.4% respectively. However, all the residues after liquefactions show higher lignin compositions than polysaccharides indicating that hemicellulose and cellulose are the major components liquefied in iron-catalyzed liquefactions.

Comparison of IR Spectra of Switchgrass with the Residue After Iron(0)-Catalyzed Liquefaction

The FT-IR spectra of switchgrass was compared with the residue after iron(0)-catalyzed liquefaction to further analyze the liquefaction process. The reflectance IR spectra of switchgrass

Table 4 The effects of different iron(0)-catalyzed liquefactions on compositions and decomposition temperatures of major components in switchgrass biomass

Entry	Catalyst and reaction conditions	Decomposition temperature °C (ΔT_{decomp})		Composition (%, w/w)		
		Hemi-cellulose and cellulose	Lignin	Hemi-cellulose and cellulose	Lignin	Ash
1	Untreated switchgrass	297–322	431	80.4	15.4	4.4
2	10% (w/w) Fe(0), H_2O, 210 °C, 24 h	276 (34)	364 (67)	32.5	37.5	20.0
3	10%(w/w) Fe(0), H_2 at 200 psi, H_2O, 210 °C, 24 h	254 (56)	349 (82)	11.5	59.6	18.9
4	10% (w/w) Fe(0) + 5% Pd/C, H_2 at 200 psi, H_2O, 210 °C, 24 h	265 (45)	345 (86)	35.8	41.3	7.9
5	10% (w/w) Fe(0) + 5% Raney-Ni, H_2 at 200 psi, H_2O, 210 °C, 24 h	250 (60)	300 (131)	3.9*	61.1*	19.0
6	10% (w/w) Fe(0) + 10% (w/w) $FeCl_3$, H_2O, 210 °C, 24 h	245 (65)	338 (93)	21.7	50.3	18.0
7	10% (w/w) Fe(0) + 10% (w/w), $FeCl_3$, 60% aq. EtOH, 210 °C, 24 h	254 (56)	313 (118)	15.4*	58.7*	15.9

* Overlap peaks

(green) and the liquefaction residue are shown from entry 2, Table 4; 10% (w/w) Fe(0), H_2O, 210 °C, and 24 h, (red) are shown in Fig. 3. The major IR absorption bands at -O–H, 3346; -C–H, 2921; -C=O, 1723; aromatic -C=C- 1596; and -C–O, 1033 cm^{-1} were assigned by comparison with switchgrass IR spectra reported in the literature [48, 49]. There are no significant changes in at -O–H, 3346; -C–H, 2921 cm^{-1} bands. However, the carbonyl absorption at 1723 cm^{-1} is greatly reduced in the liquefaction residue indicating that the ester bonds from hemicellulose fraction of switchgrass may have hydrolyzed in the liquefaction. The aromatic -C=C- absorption at 1596 cm^{-1} in residue is relatively increased in comparison to other absorptions, indicating that the lignin fraction is only mildly affected by the liquefaction. This result further confirms the thermogravimetric analysis results on percentage composition of lignin in Table 4 as well. In addition, the -C–O absorption band at 1033 cm^{-1} is relatively decreased in the residue showing the loss of polysaccharides due to liquefaction. The FT-IR spectra from other samples are included in supplementary material.

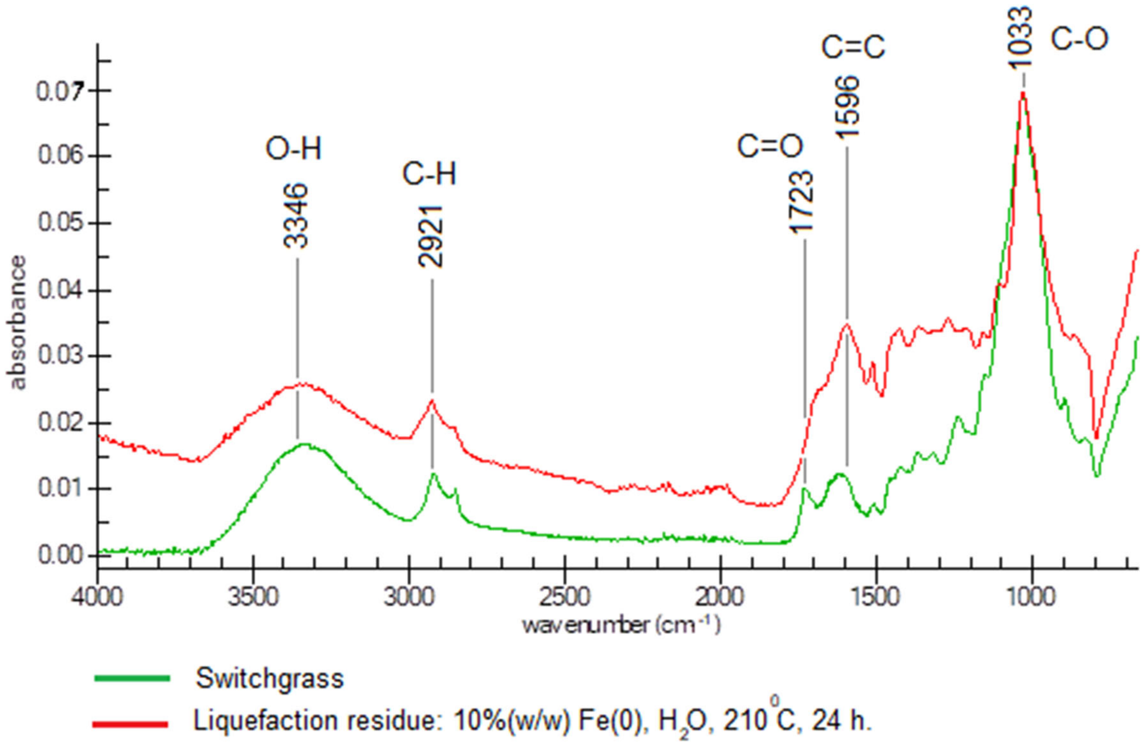

Fig. 3 Reflectance FT-IR spectra of switchgrass (green) and liquefaction residue from entry 2, Table 4; 10% (w/w) Fe(0), H_2O, 210 °C, 24 h (red)

Conclusion

The effects of a series of co-catalysts and reductive conditions were studied on the iron(0)-catalyzed hydrothermal liquefaction of untreated switchgrass. This study demonstrates the importance of decreasing the polarity of the solvent medium in improving the liquefaction yield in experiments carried out without a hydrogen atmosphere. In addition, the higher liquefaction yield in $FeCl_3$ co-catalyst-added experiment is probably due to Lewis acidity of Fe^{3+}, and Brønsted acidity of HCl formed as a result of the hydrolysis of $FeCl_3$ in water. These acidic species can catalyze the hydrolysis of glycosidic bonds in polysaccharides as well as ether bonds in lignin components in switchgrass promoting the liquefaction. Furthermore, the addition of a hydrogen atmosphere has shown a significant improvement in hydrothermal liquefaction yields of switchgrass, suggesting that the in situ hydrogen generation as shown in Eq. 1 can only play a minor contribution in the liquefaction process. Additionally, in the case of experiments carried out under a hydrogen atmosphere, the addition of Pd/C or Raney-Ni as a co-catalyst could produce only marginal improvements in liquefaction yields. However, there are significant changes in compositions of the products due to additions of these co-catalysts. This result is most likely due to facile conversion of the initially formed liquefaction products to relatively highly reduced products in the presence of better hydrogenation catalysts Pd/C or Raney-Ni. Therefore, in conclusion, the Pd/C or Raney-Ni co-catalysts are mostly involved in the reduction of the initially formed liquefaction products. The IR and thermogravimetric analysis of residues revealed that polysaccharide fraction is mainly liquefied, concluding the difficulty of depolymerization of lignin under the conditions used. We are currently working on further deoxygenation of liquefied bio-oil product to hydrocarbon fuels as well as recycling of the iron catalyst.

Funding Information This study received financial support from National Science Foundation of the United States (US-NSF) (through Grant Nos. CBET-1704144, HRD-1036593, and HRD-1914692).

References

1. Cheng JJ, Timilsina GR (2011) Status and barriers of advanced biofuel technologies: a review. Renew Energy 36(12):3541–3549. https://doi.org/10.1016/j.renene.2011.04.031
2. Alonso DM, Bond JQ, Dumesic JA (2010) Catalytic conversion of biomass to biofuels. Green Chem 12(9):1493–1513. https://doi.org/10.1039/C004654J
3. Gollakota ARK, Kishore N, Gu S (2018) A review on hydrothermal liquefaction of biomass. Renew Sust Energ Rev 81:1378–1392. https://doi.org/10.1016/j.rser.2017.05.178
4. Höök M, Aleklett K (2010) A review on coal-to-liquid fuels and its coal consumption. Int J Energy Res 34(10):848–864. https://doi.org/10.1002/er.1596
5. Mochida I, Okuma O, Yoon S-H (2013) Chemicals from direct coal liquefaction. Chem Rev 114(3):1637–1672. https://doi.org/10.1021/cr4002885
6. Ail SS, Dasappa S (2016) Biomass to liquid transportation fuel via Fischer Tropsch synthesis–technology review and current scenario. Renew Sust Energ Rev 58:267–286. https://doi.org/10.1016/j.rser.2015.12.143
7. Shui H, Cai Z, Xu C (2010) Recent advances in direct coal liquefaction. Energies 3(2):155–170. https://doi.org/10.3390/en3020155
8. Speight J (2008) Synthetic fuels handbook: properties, process and performance. McGraw Hill, NewYork
9. Shi Z, Jin L, Zhou Y, Li Y, Hu H (2017) Effect of hydrothermal treatment on structure and liquefaction behavior of Baiyinhua coal. Fuel Process Technol 167:648–654. https://doi.org/10.1016/j.fuproc.2017.08.015
10. Pedersen TH, Grigoras I, Hoffmann J, Toor SS, Daraban IM, Jensen CU, Iversen S, Madsen RB, Glasius M, Arturi KR (2016) Continuous hydrothermal co-liquefaction of aspen wood and glycerol with water phase recirculation. Appl Energy 162:1034–1041. https://doi.org/10.1016/j.apenergy.2015.10.165
11. Zhang Y (2010) Hydrothermal liquefaction to convert biomass into crude oil. Biofuels from agricultural wastes and byproducts. Wiley, NewYork
12. Kruse A, Funke A, Titirici M-M (2013) Hydrothermal conversion of biomass to fuels and energetic materials. Curr Opin Chem Biol 17(3):515–521. https://doi.org/10.1016/j.cbpa.2013.05.004
13. Behrendt F, Neubauer Y, Oevermann M, Wilmes B, Zobel N (2008) Direct liquefaction of biomass. Chem Eng Technol 31(5):667–677. https://doi.org/10.1002/ceat.200800077
14. Gollakota A, Kishore N, Gu S (2017) A review on hydrothermal liquefaction of biomass. Renew Sust Energ Rev 81:1878–1892. https://doi.org/10.1016/j.rser.2017.05.178
15. Lu Z, Zheng H, Fan L, Liao Y, Ding B, Huang B (2013) Liquefaction of sawdust in 1-octanol using acidic ionic liquids as catalyst. Bioresour Technol 142:579–584. https://doi.org/10.1016/j.biortech.2013.05.091
16. Chen H, Zhang Y, Xie S (2012) Selective liquefaction of wheat straw in phenol and its fractionation. Appl Biochem Biotechnol 167(2):250–258. https://doi.org/10.1007/s12010-012-9675-y
17. Yamada T, Ono H, Ohara S, Yamaguchi A (1996) Characterization of the products resulting from direct liquefaction of cellulose I. Identification of intermediates and the relevant mechanism in direct phenol liquefaction of cellulose in the presence of water. Mokuzai Gakkaishi 42(11):1098–1104 http://pascal-francis.inist.fr/vibad/index
18. Yamada T, Ono H (1999) Rapid liquefaction of lignocellulosic waste by using ethylene carbonate. Bioresour Technol 70(1):61–67. https://doi.org/10.1016/S0960-8524(99)00008-5
19. Wang W, Yu Q, Meng H, Han W, Li J, Zhang J (2018) Catalytic liquefaction of municipal sewage sludge over transition metal catalysts in ethanol-water co-solvent. Bioresour Technol 249:361–367. https://doi.org/10.1016/j.biortech.2017.09.205
20. Lu J, Li X, Yang R, Zhao J, Liu Y, Qu Y (2014) Liquefaction of fermentation residue of reed- and corn stover-pretreated with liquid hot water in the presence of ethanol with aluminum chloride as the catalyst. Chem Eng J 247:142–151. https://doi.org/10.1016/j.cej.2014.02.094
21. Nazari L, Yuan Z, Souzanchi S, Ray MB, Xu C (2015) Hydrothermal liquefaction of woody biomass in hot-compressed water: catalyst screening and comprehensive characterization of bio-crude oils. Fuel 162:74–83. https://doi.org/10.1016/j.fuel.2015.08.055
22. Hwang H, Lee JH, Choi I-G, Choi JW (2019) Comprehensive characterization of hydrothermal liquefaction products obtained from woody biomass under various alkali catalyst concentrations.

Environ Technol 40(13):1657–1667. https://doi.org/10.1080/09593330.2018.1427799

23. Alper K, Tekin K, Karagoz S (2019) Hydrothermal liquefaction of lignocellulosic biomass using potassium fluoride doped alumina. Energy Fuel 33:3248–3256. https://doi.org/10.1021/acs.energyfuels.8b04381
24. Chen Y, Cao X, Zhu S, Tian F, Xu Y, Zhu C, Dong L (2019) Synergistic hydrothermal liquefaction of wheat stalk with homogeneous and heterogeneous catalyst at low temperature. Bioresour Technol 278:92–98. https://doi.org/10.1016/j.biortech.2019.01.076
25. Remon J, Randall J, Budarin VL, Clark JH (2019) Production of bio-fuels and chemicals by microwave-assisted, catalytic, hydrothermal liquefaction (MAC-HTL) of a mixture of pine and spruce biomass. Green Chem 21:284–299. https://doi.org/10.1039/c8gc03244k
26. Tekin K, Akalin MK, Karagöz S (2016) The effects of water tolerant Lewis acids on the hydrothermal liquefaction of lignocellulosic biomass. J Energy Inst 89(4):627–635. https://doi.org/10.1016/j.joei.2015.06.003
27. Durak H (2019) Characterization of products obtained from hydrothermal liquefaction of biomass (Anchusa azurea) compared to other thermochemical conversion methods. Biomass Conv Biorefin 9(2):459–470. https://doi.org/10.1007/s13399-019-00379-4
28. Hao N, Alper K, Tekin K, Karagoz S, Ragauskas AJ (2019) One-pot transformation of lignocellulosic biomass into crude bio-oil with metal chlorides via hydrothermal and supercritical ethanol processing. Bioresour Technol 288:121500. https://doi.org/10.1016/j.biortech.2019.121500
29. Bi Z, Zhang J, Peterson E, Zhu Z, Xia C, Liang Y, Wiltowski T (2017) Biocrude from pretreated sorghum bagasse through catalytic hydrothermal liquefaction. Fuel 188:112–120. https://doi.org/10.1016/j.fuel.2016.10.039
30. Cheng S, Wei L, Rabnawaz M (2018) Catalytic liquefaction of pine sawdust and in-situ hydrogenation of bio-crude over bifunctional Co-Zn/HZSM-5 catalysts. Fuel 223:252–260. https://doi.org/10.1016/j.fuel.2018.03.043
31. Cheng S, Wei L, Alsowij M, Corbin F, Boakye E, Gu Z, Raynie D (2017) Catalytic hydrothermal liquefaction (HTL) of biomass for bio-crude production using Ni/HZSM-5 catalysts. AIMS Environ Sci 4(3):417–430
32. Breunig M, Gebhart P, Hornung U, Kruse A, Dinjus E (2018) Direct liquefaction of lignin and lignin rich biomasses by heterogenic catalytic hydrogenolysis. Biomass Bioenergy 111:352–360. https://doi.org/10.1016/j.biombioe.2017.06.001
33. Xu C, Etcheverry T (2008) Hydro-liquefaction of woody biomass in sub- and super-critical ethanol with iron-based catalysts. Fuel 87:335–345. https://doi.org/10.1016/j.fuel.2007.05.013
34. Xu C, Lad N (2008) Production of heavy oils with high caloric values by direct liquefaction of woody biomass in sub/near-critical water. Energy Fuel 22:635–642. https://doi.org/10.1021/ef700424k
35. Miyata Y, Yamazaki Y, Hirano Y, Kita Y (2018) Quantitative analysis of the aqueous fraction from the Fe-assisted hydrothermal liquefaction of oil palm empty fruit bunches. J Anal Appl Pyrolysis 132:72–81. https://doi.org/10.1016/j.jaap.2018.03.013
36. Miyata Y, Sagata K, Yamazaki Y, Teramura H, Hirano Y, Ogino C, Kita Y (2018) Mechanism of the Fe-assisted hydrothermal liquefaction of lignocellulosic biomass. Ind Eng Chem Res 57:14870–14877. https://doi.org/10.1021/acs.iecr.8b03725
37. de Caprariis B, Bavasso I, Bracciale MP, Damizia M, De Filippis P, Scarsella M (2019) Enhanced bio-crude yield and quality by reductive hydrothermal liquefaction of oak wood biomass: Effect of iron addition. J Anal Appl Pyrolysis 139:123–130. https://doi.org/10.1016/j.jaap.2019.01.017
38. Aysu T, Durak H (2016) Catalytic effects of borax and iron(III) chloride on supercritical liquefaction of Anchusa azurea with methanol and isopropanol. Energ Sources Part A-Recov Util Environ Effects 38(12):1739–1749. https://doi.org/10.1080/15567036.2014.958633
39. Hrcka R, Kučerová V, Hýrošová T (2018) Correlations between Oak Wood Properties. BioResources 13(4):8885–8898
40. Kaliyan N, Morey RV (2010) Densification characteristics of corn cobs. Fuel Process Technol 91(5):559–565. https://doi.org/10.1016/j.fuproc.2010.01.001
41. Kaliyan N, Morey R, White M, Doering A (2009) Roll press briquetting and pelleting of corn stover and switchgrass. Transact ASABE 52(2):543–555. https://doi.org/10.13031/2013.26812
42. Di Blasi C (2008) Modeling chemical and physical processes of wood and biomass pyrolysis. Progress Energ Combust Sci 34(1):47–90. https://doi.org/10.1016/j.pecs.2006.12.001
43. Lucas-Torres C, Lorente A, Cabañas B, Moreno A (2016) Microwave heating for the catalytic conversion of melon rind waste into biofuel precursors. J Clean Prod 138:59–69. https://doi.org/10.1016/j.jclepro.2016.03.122
44. Wiredu B, Amarasekara AS (2015) The effect of metal ions as co-catalysts on acidic ionic liquid catalyzed single-step saccharification of corn stover in water. Bioresour Technol 189:405–408. https://doi.org/10.1016/j.biortech.2015.04.030
45. Minowa T, Zhen F, Ogi T (1997) Liquefaction of cellulose in hot compressed water using sodium carbonate: products distribution at different reaction temperatures. J Chem Eng Japan 30(1):186–190. https://doi.org/10.1252/jcej.30.186
46. Zhang H, Zhang S, Yuan H, Lyu G, Xie J (2018) FeCl3-catalyzed ethanol pretreatment of sugarcane bagasse boosts sugar yields with low enzyme loadings and short hydrolysis time. Bioresour Technol 249:395–401. https://doi.org/10.1016/j.biortech.2017.10.053
47. Amarasekara AS, Deng F (2019) Acidic ionic liquid catalyzed liquefaction of untreated switchgrass biomass in acetone and Pd-La(OTf)3 catalyzed reduction of the products. Biomass Bioenergy 127:105260. https://doi.org/10.1016/j.biombioe.2019.105260
48. Yue Y, Lin Q, Irfan M, Chen Q, Zhao X, Li G (2017) Characteristics and potential values of bio-products derived from switchgrass grown in a saline soil using a fixed-bed slow pyrolysis system. BioResources 12(3):6529–6544
49. Irmak S, Meryemoglu B, Sandip A, Subbiah J, Mitchell RB, Sarath G (2018) Microwave pretreatment effects on switchgrass and miscanthus solubilization in subcritical water and hydrolysate utilization for hydrogen production. Biomass Bioenergy 108:48–54. https://doi.org/10.1016/j.biombioe.2017.10.039